Determination of the Structure of Alanine Racemase from *Bacillus stearothermophilus* at 1.9-Å Resolution[†,‡]

Jeffrey P. Shaw,[§] Gregory A. Petsko, and Dagmar Ringe*

Departments of Biochemistry and Chemistry and the Rosenstiel Basic Medical Sciences Research Center, Brandeis University, 415 South Street, Waltham, Massachusetts 02254

Received July 26, 1996; Revised Manuscript Received November 25, 1996[⊗]

ABSTRACT: The molecular structure of alanine racemase from *Bacillus stearothermophilus* was determined by X-ray crystallography to a resolution of 1.9 Å. The alanine racemase monomer is composed of two domains, an eight-stranded α/β barrel at the N-terminus, which includes residues 1−240, and a C-terminal domain essentially composed of β-strand (residues 241−388). In the structure of the dimer the mouth of the α/β barrel of one monomer faces the second domain of the other monomer. The pyridoxal 5′-phosphate (PLP) cofactor lies in and above the mouth of the α/β barrel and is covalently linked via an aldimine linkage to Lys39, which is at the C-terminus of the first β-strand of the α/β barrel. This is the first example of a PLP cofactor binding in the active site of a α/β barrel. A number of other residues are involved in maintaining the position of the PLP in the protein. Of these, Arg219 is the most interesting, as it forms a hydrogen bond with the pyridine nitrogen of the cofactor. This is the first known occurrence of such an interaction with PLP and is expected to influence the electron delocalization in the PLP-alanine intermediates. A second arginine residue, Arg136, donates a hydrogen bond to the phenolic oxygen of PLP and may be involved in the binding of substrate as well as stabilization of intermediates. Finally, Tyr265′, from the second monomer, is postulated to be 2 proton donor to the carbanion intermediate.

Gram-positive and Gram-negative bacteria require the D-isomer of alanine as an essential building block in the synthesis of the peptidoglycan layer of cell walls. The synthesis of the bacterial cell wall is believed to start with UDP-*N*-acetylmuramic acid, to which assorted free amino acids are added (Adams, 1976). UDP-*N*-acetylmuramyl-L-Ala-D-Glu-*meso*-diaminopimelate-D-Ala-D-Ala is a key intermediate in the initial stage of synthesis of the peptidoglycan layer. D-alanine is added onto the growing amino acid chain as a D-alanine dipeptide. This dipeptide is produced by two enzymes, alanine racemase (E. C. 5.1.1.1), and D-Ala:D-Ala ligase (E.C. 6.3.2.4). Alanine racemase, the first enzyme in the biosynthetic pathway of peptidoglycan synthesis, racemizes the common L isomer of alanine to the D isomer. The D-alanine dipeptide is then produced in a reaction catalyzed by D-Ala:D-Ala ligase, whose structure has recently been solved (Fan *et al.*, 1994), and the peptide is then introduced by D-Ala-D-Ala adding enzyme (E. C. 6.3.2.15) to the growing UDP-*N*-acetylmuramyl-L-Ala-D-Glu-*meso*-diaminopimelate chain.

Alanine racemase is unique to bacteria, with one known exception, an alanine racemase involved in the synthesis of cyclosporin A isolated from the fungus *Tolypocladium niveum* (Hoffmann *et al.*, 1994). The fact that the peptidoglycan biosynthetic pathway is unique to bacteria renders the enzymes in this pathway attractive targets for inhibitors, since inhibitors specific for these enzymes could potentially function as antibiotics. Alanine racemases have been isolated, at least partially purified, and characterized from several different bacteria. Alanine racemase was identified for the first time in *Streptococcus faecalis* (Wood & Gunsalus, 1951), the first purified alanine racemase was isolated from *Pseudomonas putida* (Rosso *et al.*, 1969), while partially purified enzyme was also obtained from *Bacillus subtilis* (Diven *et al.*, 1964) and *Escherichia coli* (Lambert & Neuhaus, 1972). The first mechanistic information about alanine racemase was obtained with the partially purified membrane-bound alanine racemase of *E. coli* B (Kaczorowski *et al.*, 1975a,b; Wang & Walsh, 1978). These studies also showed that alanine racemase is the target of two natural antibiotics, D-cycloserine and *O*-carbamoyl-D-serine (Neuhaus, 1967). It was subsequently discovered that many alanine analogues inhibit alanine racemase, such as β,β,β-trifluoroalanine (Faraci & Walsh, 1988), alanine phosphonate (Copié *et al.*, 1988), 1-aminocyclopropane phosphonate (Erion & Walsh, 1987), and β-chloro- and β-fluoroalanine (Wang & Walsh, 1978). These inhibitors all suffer from a lack of specificity; they also target other pyridoxal 5′-phosphate-containing enzymes. In order to design a mechanism-based inhibitor specific for alanine racemase, an understanding of the structure of the enzyme, and especially of the active site, would be helpful.

Alanine racemase from *Bacillus stearothermophilus* was cloned, and the structural gene was sequenced (Tanizawa *et al.*, 1988). The amino acid sequence greatly resembles that of alanine racemases isolated from other bacteria; it is thus expected that the structures of all these alanine racemases will be very similar. The gene has been introduced into

[†] This work was supported by NSF Grant MCB 9317373 to D.R. and, for the first year, NIH Grant GM 26788 to G.A.P. and D.R. J.P.S. was supported by Grant 823A-037105 from the Swiss National Science Foundation.

[‡] The coordinates for alanine racemase have been deposited and are available from the Brookhaven Protein Data Bank under access code 1SFT.

* Corresponding author.

[§] Present address: Geneva Biomedical Research Institute, Chemin des Aulx 14, 1228 Plan-les-Ouates, Geneva, Switzerland.

[⊗] Abstract published in *Advance ACS Abstracts,* February 1, 1997.

S0006-2960(96)01856-9 CCC: $14.00

Table 1: Data Collection Statistics for Native and Derivative Data Sets[a]

	resolution[a] (Å)	total no. of reflections $I/\sigma(I) > 1$	unique no. of reflections $I/\sigma(I) > 1$	completeness of data (%)	R_{merge}[b]	R_{iso}[c]	$I/\sigma(I)$	redundancy[d]	heavy atom salt concn (mM)	heavy atom salt soak time (h)
native set 1	25.0−2.0	86 124	38 945	77	6.2		7.2	2.2		
native set 2[e]	25.0−1.6	21 2543	62 823	62	4.4		9.3	3.4		
	10.0−1.9		52 379	83						
EMP[f]	25.0−2.5	47 985	22 342	91	5.9	0.22	10.8	2.1	1	12
HgI	25.9−2.5	51 508	20 628	70	8.6	0.27	5.9	2.5	1	16
PIP[g]	25.0−2.5	45 483	19 791	68	8.6	0.23	6.4	2.3	2	16

[a] All derivative data were used at resolutions of 20−2.5 Å, and the values in this table represent data within those cutoffs. [b] $R_{merge} = \sum\sum_i |I_i \langle I \rangle| \sum \langle I \rangle$, where I_i is the scale factor-corrected intensity for a reflection and $\langle I \rangle$ is the mean intensity for that reflection. [c] Mean fractional isomorphous difference, $R_{iso} = \sum(|F_{PH}| - |F_P|)/\sum(|F_P|)$, where F_{PH} and F_P are the derivative and native structure factor amplitudes, respectively. [d] Total reflections collected/unique reflections. [e] Second native data set, collected on two different orientations of the same crystal. [f] Ethyl mercury phosphate. [g] Di-μ-iodobis(ethylenediamine) diplatinum(II) nitrate.

various *E. coli* expression systems, the enzyme purified from *E. coli* cells, and the kinetic behavior studied (Inagaki *et al.*, 1986). The enzyme is a dimer of identical subunits, each with a molecular mass of 43 341 Da. Each subunit contains 388 amino acids and is known to contain a covalently bound pyridoxal 5′-phosphate cofactor. A preliminary report concerning the crystallization of alanine racemase has been published (Neidhart *et al.*, 1987). Here, we report the three-dimensional structure of alanine racemase and propose a mechanism for catalysis.

EXPERIMENTAL PROCEDURES

Purification. *Bacillus stearothermophilus* alanine racemase was expressed in *E. coli* W3110 containing the plasmid construct pMDalr3 described in Neidhart *et al.* (1987). The protein was also purified according to the procedure described in Neidhart *et al.* (1987) with Pharmacia DEAE-Sephacel replacing the DEAE-Toyopearl 650M resin and with the addition of a hydrophobic interaction chromatographic purification step at the end of the procedure.

Kinetic Measurements. Alanine racemase was assayed in the D-alanine to L-alanine direction in the manner described by Faraci and Walsh (1988). The assay was performed in 100 mM CHES buffer (pH 9.1) containing 1 mol of NAD^+, 0.072 unit of L-alanine dehydrogenase (1 unit is defined as the amount of protein which will convert 1 μmol of L-alanine to pyruvate and NH_3/min at pH 10 and at 25 °C), and concentrations of D-alanine varying between 30 and 0.4 mM, in a final volume of 200 μL. The concentration of alanine racemase was 1 nM. The reaction was started by the addition of the L-alanine dehydrogenase, and the rate was monitored on a Molecular Devices SoftMax 96-plate reader spectrophotometer at a wavelength of 340 nm. All measurements were performed 5 times. All chemicals were obtained either from Fluka AG (Buchs, Switzerland) or Sigma Chemical Co. (St. Louis, MO). Concentrations of inhibitors were between 50 and 250 mM for acetate and between 5 and 25 mM for propionate.

Crystallization. Alanine racemase was dialyzed against 1 L of 100 mM Tris-HCl buffer (pH 8.5) containing 10 μM PLP.[1] The protein was then concentrated to 30 mg/mL in Amicon concentrators (10-kDa cutoff). Large crystals of alanine racemase (1.2 mm × 1.2 mm × 0.4 mm) were grown by the hanging drop method. The hanging drop contained 10 μL of protein solution at 30 mg/mL and 10 μL of a solution containing 30% (w/v) PEG [poly(ethylene glycol)] 4000, 200 mM sodium acetate, and 100 mM Tris-HCl (pH = 8.5). Drops were equilibrated against 700 μL of the latter solution. Somewhat larger crystals were obtaining using the sitting drop method with the same conditions (the initial volume of the sitting drop was 50 μL). The crystals have a distinctive yellow color, indicating the presence of a covalently bound pyridoxal 5′-phosphate in the active site of alanine racemase. The protein crystallized in space group $P2_12_12_1$ with unit cell dimensions $a = 98.59$ Å, $b = 90.13$ Å, $c = 85.13$ Å, α, β, and $\gamma = 90^o$. There are two protein molecules per asymmetric unit, with a calculated solvent content of 45%. Since alanine racemase from *B. stearothermophilus* is a homodimer (Inagaki *et al.*, 1986), it was assumed that there was one dimer of alanine racemase in the asymmetric unit, which was subsequently confirmed.

Data Collection and Processing. When the first crystals of alanine racemase were exposed to X-ray radiation, the crystals ceased to diffract very rapidly. It was discovered that the crystals are very sensitive to temperature and rapidly become disordered at 4 °C, the standard temperature for data collection. It is interesting to note that the crystals fully regained their diffracting qualities if allowed to return to room temperature. All data sets were therefore collected at room temperature using Cu Kα radiation ($\lambda = 1.5418$ Å) using a R-axis IIC Image plate detector system mounted on a Rigaku RU-200 rotating anode generator operating at 150 kV and 40 mA. One crystal was used per data set. A second native data set was collected on the same crystal in two different orientations, in order to increase the completeness of the data set. Heavy atom derivative data sets including anomalous data were collected to 2.5-Å resolution. All data were integrated, scaled, reduced, and merged using the PROCESS package (Rigaku, Japan).

Structure Determination. The structure of alanine racemase was solved by the method of multiple isomorphous replacement (MIR) using the heavy-atom derivatives listed in Table 1. The PROTSYS package of programs was used for all calculations unless otherwise noted. The initial electron density maps were determined using the single-orientation native data set, which was 77% complete from 20 to 2.0 Å. Heavy atom positions for the EMP derivative were determined from an isomorphous difference Patterson map and confirmed by the program SHELX (Sheldrick,

[1] Abbreviations: PIP, di-μ-iodobis(ethylenediamine) diplatinum(II) nitrate; PLP,pyridoxal 5′-phosphate; EMP,ethyl mercury phosphate; BSAR, *Bacillus stearothermophilus* alanine racemase; DGD,2,2-dialkylglycine decarboxylase; TPL,tyrosine:phenol lyase; L-Asp-AT, L-aspartate aminotransferase; DAAT, D-amino acid aminotransferase.

Table 2: Heavy-Atom Parameters and Phasing Statistics

derivative	site	x^a	y	z	B^b (Å)	occupancy	monomer
EMP[c]	EMP1	0.782	0.532	0.783	21.8	0.14	1
	EMP2	0.791	0.811	0.035	23.6	0.13	2
	EMP3	0.781	0.308	0.236	28.0	0.11	2
	EMP4	0.759	0.045	0.631	26.4	0.11	1
	EMP5	0.758	0.095	0.117	25.0	0.09	2
	EMP6	0.761	0.806	0.657	23.8	0.08	1
	EMP7	0.807	0.757	0.676	19.3	0.06	1
	EMP8	0.800	0.054	0.077	19.9	0.06	2
HgI	HgI1	0.830	0.287	0.226	18.0	0.14	2
	HgI2	0.810	0.757	0.678	37.9	0.17	1
	HgI3	0.801	0.028	0.666	17.1	0.13	1
	HgI4	0.806	0.054	0.079	32.8	0.15	2
	HgI5	0.756	0.809	0.650	35.5	0.06	1
	HgI6	0.795	0.813	0.039	25.0	0.09	2
	HgI7	0.784	0.531	0.781	37.0	0.18	1
PIP[d]	PIP1	0.043	0.197	0.987	30.0	0.06	1
	PIP2	0.144	0.609	0.651	30.0	0.02	2

[a] Fractional atomic coordinates. [b] Isotropic temperature factor. [c] Ethyl mercury phosphate. [d] Di-μ-iodobis(ethylenediamine) diplatinum(II) nitrate.

1985). Positions for the heavy atoms of the other derivatives were located on difference Fourier maps and confirmed with difference Patterson maps and the program SHELX. The anomalous scattering contributions of the EMP and PIP derivatives were both used to assign the correct hand to the data and also used in subsequent protein phasing calculations. Heavy atom refinement (Table 2) followed by calculation of protein phases at 2.8 Å resolution yielded an overall mean figure of merit of 58%, which improved to 82% upon solvent flattening (a solvent content of 35% was used) with the program SQUASH (Zhang, 1993). The quality of the electron density map obtained at 2.8-Å was quite good but was improved with one round of noncrystallographic 2-fold averaging using the program RAVE (Jones 1992; Kleywegt & Jones, 1994). The orientation of the noncrystallographic 2-fold axis had been determined previously, using the locations of the heavy atoms of the EMP derivative, and the programs TOSS (Hendrikson, 1979; program modified by G. A. Petsko) and O (Jones *et al.*, 1991). The structure was built into the interpretable regions of electron density as polyalanine using the program O, and the phases were improved by combining the heavy-atom derived phases with those calculated from the polyalanine structures with the program COMBINE (Kabsch *et al.*, 1990; program modified by G. A. Petsko). The building of the polyalanine chain was greatly assisted by the secondary structure prediction of alanine racemase provided by B. Rost (personal communication; Rost & Sander, 1993, 1994). At this point, the model of only one monomer was built. This model was built into the electron density of whichever monomer in the asymmetric unit provided the better quality electron density map. The coordinates of the other monomer were calculated through the use of the noncrystallographic 2-fold axis. A total of 12 rounds of model building and phase improvement yielded the structure of both monomers containing two polyalanine chains of 323 amino acids. Positional refinement with the program XPLOR (Brünger, 1992), using very high noncrystallographic symmetry constraints gave an initial *R*-factor of 41.2% for all the data from 10- to 2.8-Å resolution. The side chains for the 323 amino acid residues were fitted into the model and the model was submitted to a round of refinement by simulated annealing and positional refinement using the program XPLOR. The resulting *R*-factor was 32.2%. The electron density maps which were examined in the subsequent cycles of refinement were calculated with coefficients $(3|F_o| - 2|F_c|)$ and $(|F_o| - |F_c|)$ in the resolution range of 10−2.5 Å. After several cycles of XPLOR positional refinement and model building, the *R*-factor decreased to a value of 27.8% for the 21 670 reflections between 10 and 2.5 Å. At this point, the data to 2.0 Å were included, and the high noncrystallographic symmetry constraints in XPLOR were removed, to yield, after a further round of simulated annealing and positional refinement, an *R*-factor of 26.6%.

Table 3: Refinement Statistics

resolution	10.0−1.9 Å
unique reflections $[I/\sigma(I)] > 1]$	52 379
completeness (%)	83
final *R*-factor (%)	19.1
free *R*-factor[a] (%)	26.7
deviations	
bond lengths (Å)	0.019
bond angles (deg)	3.42
B-factors (individual *B*-factor model)	
average, main chain (Å^2)	28.2
average, side chain (Å^2)	31.3
waters (Å^2)	32.8
total number of protein atoms	6083
total number of water molecules	212
total number of cofactor atoms	15
total number of acetate atoms	8

[a] Calculated using 5% of total reflections.

From this point on the model was refined against the higher resolution and more complete second native data set (Table 3). After a single round of model building, simulated annealing and positional refinement, group *B*-factor refinement, and individual isotropic *B*-factor refinement using standard restraints against data between 10 and 2.0 Å (44 717 reflections), the *R*-factor dropped to 23.2%. At this point, obvious water molecules were built into the model. Several more cycles of refinement of the model, using simulated annealing omit maps and positional refinement, yielded the final model. This final model, containing residues 2−383 of the first monomer and residues 2−381 for the second, refined against all data between 10 and 1.9 Å with $I > 1\sigma(I)$ (52 379 reflections), 212 water molecules, 6083 non-hydrogen protein atoms, 15 non-hydrogen PLP atoms, and 8 non-hydrogen acetate atoms, has an *R*-factor of 19.1% and root mean square (rms) deviations from ideality for bond lengths and angles of 0.019 Å and 3.42°. The electron density for the N-terminal methionine was lacking in both monomers of the dimer. At the C-terminal end, in one monomer, electron density was lacking for residues 384−388, while in the second, electron density for residues 382−388 was lacking. The corresponding amino acids were not modeled.

Heavy-Atom Sites. There are four cysteine residues per monomer of alanine racemase. The heavy atoms of the two mercurial heavy atom derivatives bound exclusively to cysteine side chains. All of the EMP and HgI atoms are near three of these cysteines, either Cys201, Cys311, or Cys358, while none bound near Cys315. Each monomer bound four EMP molecules, the other four being related to the first by a noncrystallographic 2-fold rotation axis relating the two monomers within the asymmetric unit. In fact, the orientation of the noncrystallographic 2-fold rotation axis was determined from the positions of the EMP binding sites and

permitted the 2-fold averaging performed on the initial electron density map. EMP molecules would appear to bind to Cys358 on either side of the sulfur. The occupancies of these EMP molecules (EMP6 EMP7 on monomer 1, EMP5 EMP8 on monomer 2) are substantially lower than those for the other EMP molecules. HgI molecules 2, 4, 5, and 6 bind to sites common to EMP sites. However, HgI molecules 1 and 3 bind to Cys311 at a new site. These mercury binding sites all lie within the monomer−monomer interface. The PIP molecules (which bind in positions related by noncrystallographic symmetry) bind between the side chains of Met375 and Arg52. They would appear to bind preferentially to the methionine side chain.

Crystal Packing. The longest axis of the alanine racemase dimer lies approximately along the *y* axis of the unit cell. The length of this long axis is 88 Å, which corresponds well to a length of 90.1 Å for the *y* axis of the unit cell. The width of the dimer is 52 Å wide, which corresponds to the unit cell *x* axis, and the height of a monomer is approximately 42 Å and corresponds to the *z* axis of the unit cell. The monomer long axis is also roughly aligned along the *y* axis. When viewed along the crystallographic *z* axis, the second domain of the monomer is aligned almost exactly with the *y* axis, whereas the axis of the barrel in the α/β barrel is approximately 55° off the crystallographic *y* axis toward the *x* axis. There is thus an angle of approximately 125° between the α/β barrel and the second domain. The α/β barrel is approximately 45 Å in diameter, whereas the second domain is approximately 65 Å long. The packing of the dimers is extremely dense, with a very small number of narrow solvent channels running roughly along the crystallographic *y* and *z* axes, with no evidence of any channels in any other direction. While there are contacts between different dimers in the crystal, there is no evidence of any hydrogen bond or salt bridge interactions between different dimers.

Crystal Form. The crystals of alanine racemase obtained under the conditions described above are different from those obtained by Neidhart *et al.*, (1987). The crystals described by Neidhart *et al.* (1987) were in space group $P2_1$, with the values of α, γ, and especially β being equal to 90° within experimental error. Some of these crystals apparently displayed *mmm* Laue symmetry, while others displayed *2/m* symmetry, with varying degrees of similarity to the *mmm* pattern. It was therefore postulated that the crystals suffered from varying degrees of twinning by pseudomerohedry of order 2, this twinning facilitated by the fact that $\beta = 90°$. The crystals described in this paper are of space group $P2_12_12_1$, with unit cell angles being defined as 90°, and with unit cell dimensions of a = 98.6 Å, b = 90.2 Å, and c = 85.2 Å. It would appear that the slightly different crystallization conditions resulted in crystals of higher symmetry. Furthermore, the unit cell dimensions are very similar, with the *b* axis in the new crystals corresponding to the c axis in the Neidhart crystals (90.2 Å vs 89.9 Å) and the *c* axis in the new crystals corresponding to the *a* axis in the Neidhart crystals (85.2 Å vs 85.2 Å). The length of the *a* axis in the new crystal form is 10% shorter than the corresponding unit cell length (*b* axis) in the Neidhart crystals (98.6 Å vs 110.0 Å). The difference in symmetry and unit cell length also suggested that there is one dimer in the asymmetric unit of the new crystal form, as opposed to two in the Neidhart crystal form. The reason why alanine racemase crystallized in these two different forms became apparent, once the structure was well-defined.

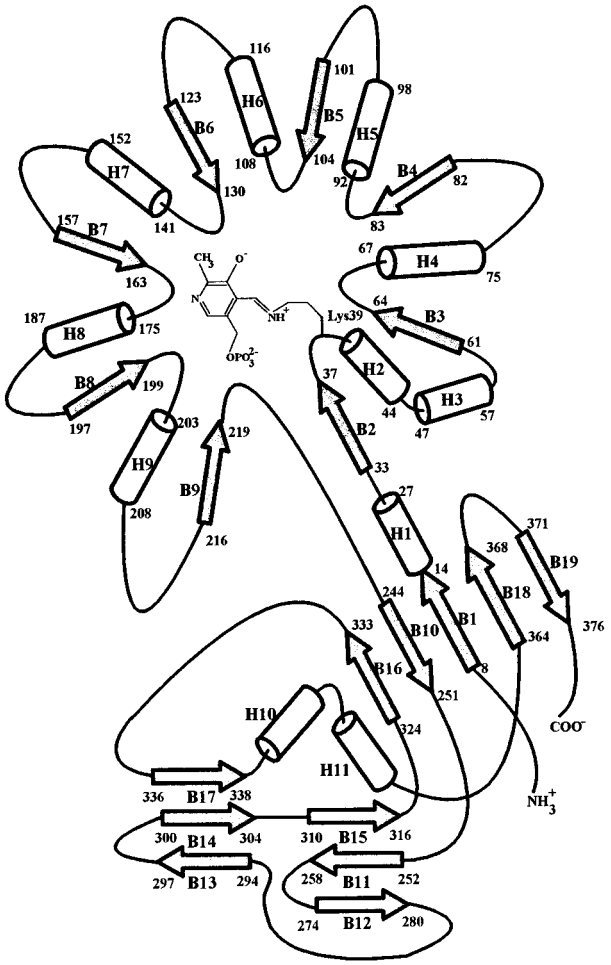

FIGURE 1: Schematic diagram of the secondary structure of alanine racemase.

RESULTS

Description of the Structure. The alanine racemase monomer is composed of two domains (see Figures 1 and 2). The N-terminal domain, comprising residues 1−240, is an eight-stranded αA/Bβ barrel containing β-strands B2−B9 and α-helices H1−H9. The first β-strand of the monomer (B1) is not strictly part of the α/β barrel since it is at the extreme N-terminal end of the protein and forms hydrogen bonds with a long β-strand at the C-terminal end of the α/β barrel which connects the two domains (B10). Likewise, the first α-helix of the α/β barrel domain is not strictly part of the barrel. The first β-strand of the α/β barrel comprises residues His33 to Val38 (B2). Lys39, which is covalently linked to the PLP cofactor through its Nζ atom, lies at the C-terminal end of this first β-strand of the barrel and is the first residue of an α-helix composed of residues Lys39−Gly44 (H2). The final β-strand of the α/β barrel is followed by a long β-strand, which hydrogen-bonds to the N-terminal strand (B1) and to a β-strand in the second domain (B16). This long strand connects the C-terminus of the α/β barrel with the N-terminus of the second domain. This second domain (the C-terminal domain) of the alanine racemase monomer is essentially composed of β-strand (residues 240−388), with the exception of two short α-helices (H10 and H11). This second domain does not appear to present a

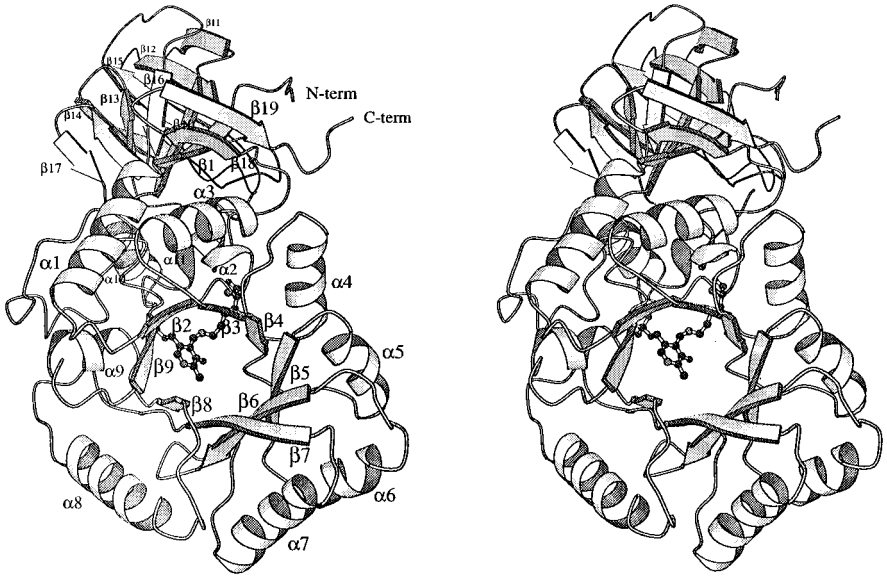

FIGURE 2: Stereo ribbon diagram of the alanine racemase monomer. Every tenth residue is marked.

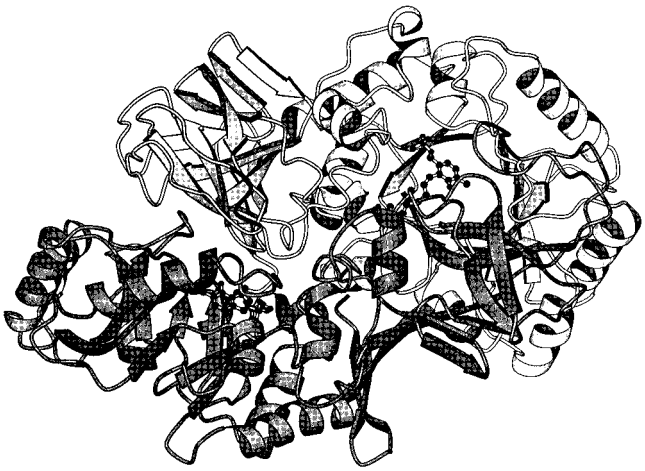

FIGURE 3: Ribbon diagram of the alanine racemase dimer. The loops marked in black contain the residues that play an important role in the active site of the opposite monomer (residues 265−269).

Table 4: Polar Interactions (Hydrogen Bonding and Salt Bridge) at the Interface between Monomers of the Alanine Racemase Dimer[a]

residue from monomer 1	residue from monomer 2	distance (Å)
Arg 107 NH1	Val 254 O	3.2
Arg 107 NH1	His 253 NE2	3.0, 3.8
Gly 138 O	His 253 NE2	3.3
Arg 136 O	Thr 279 OD1	2.7
Met 134 O	Ser 264 N	2.7, 6.3
His 166 NE2	Tyr 265 OH	3.0
Ala 168 O	Gly 266 N	3.1
Leu 349 O	Arg 291 NH2	3.1, 6.4
Arg 89 NH1	Phe 4 O	2.8
Arg 89 NE	Asp 7 OD1	3.2
Asp 92 OD2	His 5 ND1	3.07
Asp 68 OD2	Asn 379 OD1	3.0, 4.3
Glu 69 OE2	Arg 363 NH1	2.9
Arg 290 N	Glu 355 OE2	3.1

[a] In some cases, the interaction is only seen for one subunit pair and not the other. Both distances are given for these cases.

readily identifiable motif and shares little similarity with other known structures.

The alanine racemase dimer (Figure 3) is formed by interactions between the N-terminal domain of one monomer with the C-terminal domain of its partner. Both monomers of the homodimeric alanine racemase are very similar, with a mean rms deviation of the α-carbon positions of the two monomers of 0.29 Å. There are a few obvious polar interactions between the two monomers (Table 4); however, it would appear that hydrophobic interactions play an important role in maintaining the dimer structure.

During the refinement of the structure, several important inconsistencies between the published amino acid sequence of alanine racemase (Tanizawa *et al.*, 1988) and the electron density observed in simulated annealing omit maps became apparent. Most noticeably, Gly286 and its two neighboring residues had adopted a conformation which did not fit well into the main-chain density. There was a very large side-chain electron density for this glycine residue, corresponding very well with that expected for the indole group of a tryptophan residue. Examination of the multiple sequence alignment of alanine racemases from different bacteria (Tanizawa *et al.*, 1988) showed that the three other alanine racemases had either a tryptophan or tyrosine residue in this position, and that a gap had been introduced in the sequence of the alanine racemase from *B. stearothermophilus* in order to maximize the sequence similarities. A tryptophan residue was therefore introduced after Gly286. The electron density for residues 57−61 also did not correspond to the expected amino acid residues. On the basis of the sequencing of the structural gene, residue 57 was expected to be an arginine. There was no electron density for the arginine side chain at this position, nor was there any room for such a side chain, since it was in a small hydrophobic pocket. This residue was therefore maintained as an alanine residue. The electron density confirmed the absence of any side-chain density for Gly58. In the case of Pro59, there was suitable electron density for a proline residue, but there also appeared to be another residue, between Gly58 and Pro59. An amino acid backbone was inserted at this point, on the C-terminal side of Gly58. Upon refinement, the electron density suggested that this amino acid could actually be an alanine. Examination of the sequence alignment (Tanizawa *et al.*, 1988) indicated that this alanine residue was conserved among at least four alanine racemases. Proline 60 was obviously not

```
                    MNDFHRDTWAEVDLDAIYDNVENLRRLLPDDTHIMAVVKANAYGHGDVQV    50

old sequence        ARTALERGPPP AVAFLDEA
                    |||||| |    ||||||||
                    ARTALEAGASRLAVAFLDEALALREKGIEAPILVLGASRPADAALAAQQR   100

                    IALTVFRSDWLEEASALYSGPFPIHFHLKMDTGMGRLGVKDEEETKRIVA   150

                    LIERHPHFVLEGLYTHFATADEVNTDYFSYQYTRFLHMLEWLPSRPPLVH   200

                    CANSAASLRFPDRTFNMVRFGIAMYGLAPSPGIKPLLPYPLKEAFSLHSR   250

old sequence                                        YADG VRRL
                                                    |||| |||
                    LVHVKKLQPGEKVSYGATYTAQTEEWIGTIPIGYADGWLRRLQHFHVLVD   300

                    GQKAPIVGRICMDQCMIRLPGPLPVGTKVTLIGRQGDEVISIDDVARHLE   350

                    TINYEVPCTISYRVPRIFFRHKRIMEVRNAIGRGESSA               388
```

FIGURE 4: Sequence of alanine racemase from *Bacillus stearothermophilus*. The new amino acid sequence is shown in boldface type. The old sequence is shown for the regions in which differences were observed.

a proline, since there was electron density for a long side chain. This residue was therefore replaced with a glutamine, which corresponded very well to the electron density and, furthermore, formed a hydrogen-bonding network with a water molecule (2.5 Å), which also binds to the Oϵ1 of Glu161 (2.9 Å). The sequencing had also identified residue 61 as a proline residue. However, the electron density did not correspond very well, and there was significant electron density suggesting the presence of a side chain. The electron density corresponded very well with a leucine side chain, and the proline was replaced by this leucine. This leucine side chain lies in a very hydrophobic pocket containing the side chains of Ile78, Ile82, Leu55, Val38, and Ala51. Parts of the structural gene of alanine racemase were sequenced again to confirm these substitutions or insertions. Sequencing of the structural gene for alanine racemase confirmed the two insertions (Ala59 and W288) as well as the identities of residues 57, 60, 61, and 62 (see Figure 4). The glutamine residue which had replaced Pro60 (now residue 61), was actually an arginine residue, and Pro59 was actually Ser60. The sequencing also showed that residue 289 was not a valine, but a leucine; this was confirmed by the electron density. The numbering of the amino acids in the discussion that follows is that of the new modified sequence, with a total of 388 amino acid residues per monomer.

The Active Site. The active site of alanine racemase is composed of pyridoxal 5′-phosphate, the PLP-binding residue, Lys39, and the amino acids in the immediate environment of the pyridoxal cofactor. As mentioned previously, Lys39 is at the C-terminal end of the first β-strand of the α/β barrel. The Lys side chain points toward the center of the barrel. However, the Lys39 C atom is located in the part of the barrel which is also adjacent to the second domain of the monomer (see Figures 3 and 5). The second domain of the monomer is inclined approximately 55° away from the axis of the barrel and toward the other monomer, thereby forming an angle of 125° between the two domains. The Lys39 residue is therefore not only in the α/β barrel but also in a cleft formed by the two domains of the monomer. The second domain of the second monomer lies on top of the barrel of the first monomer, so Lys39 also lies between the two monomers.

The PLP moiety lies in the approximate center of the barrel, and slightly above it, closer to the second domain of the other monomer, not toward bulk solvent. The phosphate group forms several hydrogen-bonding interactions with residues of the same monomer (see Figure 5). One of the free oxygen atoms (OP1) of the phosphate group forms a hydrogen bond with the hydroxyl oxygen of Tyr43 (2.9 Å), which is part of the helix from which Lys39 originates. The hydroxyl oxygen of Tyr354 also forms a hydrogen bond (3.0 Å) with another of the free oxygen atoms (OP2) of the phosphate group of PLP, as does the O of Ser204 (2.8 Å) with the third free oxygen atom of the phosphate group (OP3). OP2 also forms hydrogen bonds with two water molecules (at 2.8 Å), one of which also interacts with the ND2 of Asn203 (3.0 Å). This important hydrogen-bonding system renders the position of the phosphate group of the PLP rather immobile.

The environments on either side of the pyridine ring of the pyridoxal group would appear to be rather different. The side of the pyridine ring which is in contact with the α/β barrel (as opposed to that which faces the dimer interface) contains several nonpolar residues, no charged residues, and no water molecules (see Figure 6). Notably, Leu85 lies on the nonpolar side of the pyridine ring, more or less across the face of the heteroaromatic ring system, and at a distance of 3.8 Å from it. Val37 also lies on this side of the heteroaromatic ring, at a distance of 4.0 Å from the ring, while several other residues contribute to the nonpolar environment of this side of the PLP ring (Ala63, Ala65, Leu83, and Tyr164).

The other side of the pyridine ring contains a large number of charged residues, several water molecules, a lengthy hydrogen-bond network, and no nonpolar residues. The pyridine ring is held in place by an important hydrogen bond between the N1 atom of the pyridine ring and the NE of Arg219. The plane of the guanidinium group of Arg219 is perpendicular to the plane of the pyridine ring and the NE of Arg219 is 2.9 Å from the N1 atom, suggesting that there is one proton between the two, donated by the Arg219 guanidinium group. This guanidinium group is part of a long hydrogen-bonding network involving Tyr265′ (from the other monomer)-His166-Arg219-His200-His127 and Glu161 (see Figure 6). The two other nitrogen atoms of the guanidinium group of Arg219 also form hydrogen bonds, thereby fixing the position of this guanidinium group very tightly. The NH2 would appear to form a hydrogen bond with the main-chain O of Thr165 (2.9 Å) and with the ND1 of His166 (3.1 Å). This His166 lies on top of the heteroaromatic ring of the

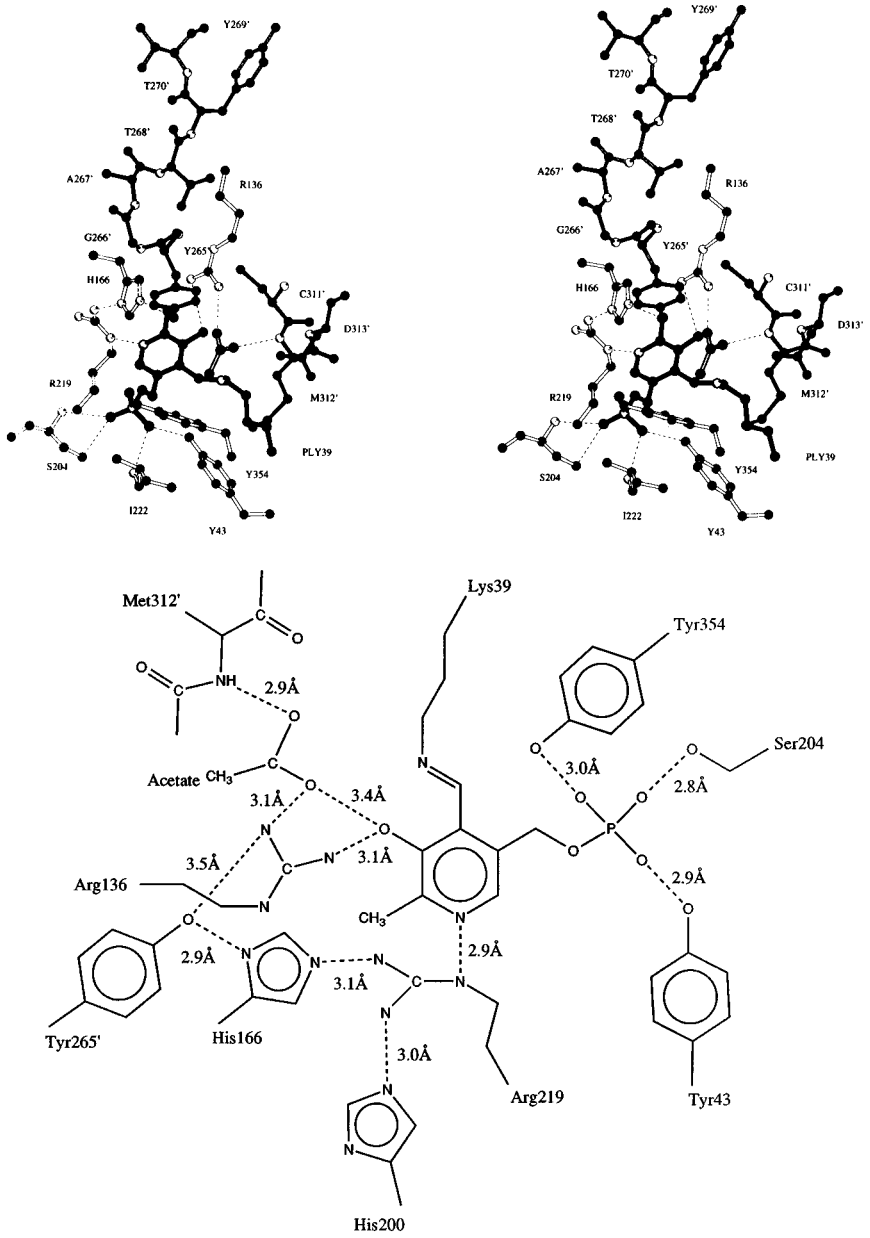

FIGURE 5: (a) Stereo diagram of the active site of alanine racemase. PLY 39 is lysine 39 with the cofactor covalently bound. (b) Schematic diagram of the active site of alanine racemase. No hydrogen atoms are shown since the protonation states of all groups are not known. Diagram not to scale. Residues labeled with a prime are from the other monomer. Dashed lines indicate presumed hydrogen bonds based on the distance between heteroatoms.

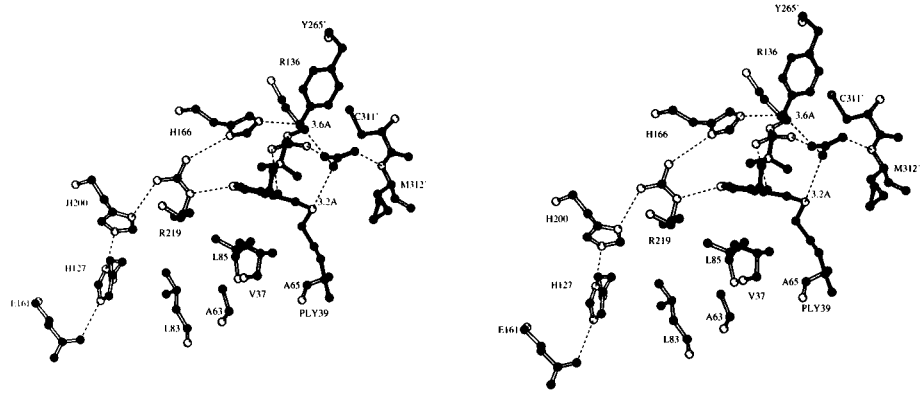

FIGURE 6: Stereo diagram of the hydrogen-bond network holding Tyr265′ and Arg219 in place. Residues labeled with a prime are from the other monomer. Distances of less than 3.5 Å are indicated by dashed lines. In general, these indicate hydrogen bonds. The dashed line between the methyl group of acetate and the NZ of the K39-PLP group indicates a close contact.

PLP molecule, its ring system almost parallel to that of the pyridine ring. His166 forms a hydrogen bond not only with the NH2 of Arg219 but also with the OH group of Tyr265′ (2.9 Å). Tyr265′ may also interact with the NH1 of Arg136

(3.3 Å). This Tyr265′ is one of the residues of the other monomer which would appear to play a role in the active site. On the other side of Arg219, the NH1 of Arg219 forms a hydrogen bond with the Nδ1 of His200 (3.0 Å). The Nϵ2 of the latter forms a hydrogen bond with the ND1 of His127 (3.2 Å). The NE2 of the latter forms a hydrogen bond with the OE2 of Glu161. This Glu161 forms a hydrogen bond to the NH1 of Arg61.

The NH2 of the guanidinium group of Arg136 forms a hydrogen bond with the phenolic oxygen (O3′) of the pyridoxal 5′-phosphate ring (3.1 Å). The NH1 group of Arg136 forms a hydrogen bond with an acetate molecule whose presence in the active site is due to the 200 mM sodium acetate in the crystallization conditions. Thus Arg136 forms a bridge between this acetate molecule and the O3′ of PLP. The guanidinium group of Arg136 is also quite close to the OH group of Tyr265′ (3.3 Å). Gln314′ is within hydrogen-bonding distance of a water molecule (3.2 Å), which itself hydrogen-bonds to the O3′ of the PLP ring (2.8 Å). Whether the interaction of Arg136 with the acetate molecule resembles that with the alanine substrate is not certain but very likely.

There are several residues from the other monomer which are close enough to the pyridoxal 5′-phosphate to play some role in binding or catalysis. The Tyr265′ mentioned above is one of these residues, and its possible role will be discussed below. Two other residues may be important, Asp313′ and Gln314′. These are part of a three-stranded antiparallel β-sheet (composed of B11, B12, and B15) in the second domain of the other monomer. The side chain of Asp313′ lies close to the N of Lys39, the OD2 atom lying 4.2 Å from the N atom. Thus, the side chain of Asp313′ could form a hydrogen bond with the free Lys39 side chain when alanine is bound in the active site. The side-chain OE1 of Gln314′ forms a hydrogen bond with the NH1 of Arg136 (2.8 Å), at least in the case of one monomer. It also interacts with a pair of water molecules, one of which also forms hydrogen bonds with the hydroxyl group of the pyridine ring of PLP. These three residues from the other monomer either maintain the positions of certain residues in the active site (notably Arg136) or may be implicated in the binding of the substrate (Asp313′ and/or Gln314′).

The crystallization of alanine racemase requires the presence of acetate in the crystallization solution. Under identical conditions lacking the 200 mM sodium acetate, the protein crystallizes far more slowly and the crystals are of very poor quality. We expect these latter crystals to be in space group $P2_1$ and to be essentially the same as those produced by Neidhart *et al.* (1987). Furthermore, an electron density near the NE of Lys39 was interpreted as being an acetate molecule (see Figures 5 and 6) which presumably binds in the active site in much the same was as alanine would be expected to do. The carboxylate of the acetate molecule is presumably binding in the site normally occupied by the carboxylate of alanine. This would bring the expected position of the amino group of alanine in very close proximity to the Nζ atom of Lys39. The carboxylic acid end of the acetate molecule forms important interactions with several atoms. One carboxylate oxygen forms a hydrogen bond with the main-chain nitrogen of Met312′ from the other monomer. The other carboxylate oxygen forms hydrogen bonds to the NH1 of Arg136 (3.1 Å) and perhaps to the O3′ phenolic group of PLP (3.4 Å). The fact that the main chain of the second domain of the other monomer is important for binding of acetate suggests a role for the second domain of alanine racemase. Furthermore, the presence of this acetate molecule in the active site of the crystallized protein suggests that acetate may be an inhibitor of the protein. The measurement of the effect of acetate on the racemization of D-alanine by alanine racemase showed that acetate is indeed a competitive inhibitor, with a K_I of 37 ± 8 mM. This result prompted the examination of the possible inhibitor properties of other small-chain carboxylic acids. Propionic acid, which resembles alanine more closely than acetate, is a much stronger inhibitor of alanine racemase, with a K_I of 41 ± 11 μM. Butyric acid was a much poorer inhibitor and was not a competitive inhibitor of alanine racemase but a perfect noncompetitive inhibitor of the enzyme. Butyric acid thereby binds just as well to the free enzyme as to the enzyme−substrate complex, implying that it is not recognized by the active site as a potential substrate. These results suggest that the size of the binding pocket for alanine is rather restrictive and cannot allow efficient binding of substrate analogues that are larger than the propionate backbone of alanine, while smaller compounds can be recognized, albeit with much lower affinity.

The difference in crystallization conditions, coupled with the presence of an acetate molecule in the active site of alanine racemase, suggests that the protein undergoes a conformational change when acetate is present. This conformational change would also occur upon binding of the substrate and suggests that the observed structure of alanine racemase represents a closed form of the protein. A conformational change upon binding of substrate is frequently observed among PLP-containing enzymes (Almo *et al.*, 1994) and generally sequesters the active site from the surrounding aqueous environment, thereby allowing the PLP chemistry to occur without secondary reactions due to the presence of water. The presence of two distinct domains in alanine racemase linked by a long tether suggests that an interdomain movement produces the closed form of the enzyme, although a movement between the two monomers could also result in a closed form of the enzyme and cannot be ruled out.

DISCUSSION

The presence of an eight-stranded α/β barrel in the structure of alanine racemase was unexpected, although with hindsight, the secondary structure prediction, performed by B. Rost using the PHD software package (Rost *et al.*, 1993, 1994), did suggest such a secondary structure motif. This is the only example of a pyridoxal 5′-phosphate molecule bound to an α/β barrel, although a large number of other cofactors (assorted metal ions, flavin nucleotides, iron−sulfur clusters, etc.) have been associated with α/β barrels (Farber & Petsko, 1990). The binding site of the pyridoxal 5′-phosphate in the active site of the α/β barrel (to Lys39) is also like that of all other α/β barrels, namely, at the C-terminal end of the barrel and at a loop connecting a β-strand to one of the external α-helices. The observation confirms the remarkable catalytic qualities of the C-terminal loops of the α/β barrel structure. A structural similarity search, based on the novel structure of alanine racemase, was undertaken by L. Holm (private communication) using the Dali software package (Holm *et al.*, 1992, 1993). The proteins whose structures are most similar to the N-terminal

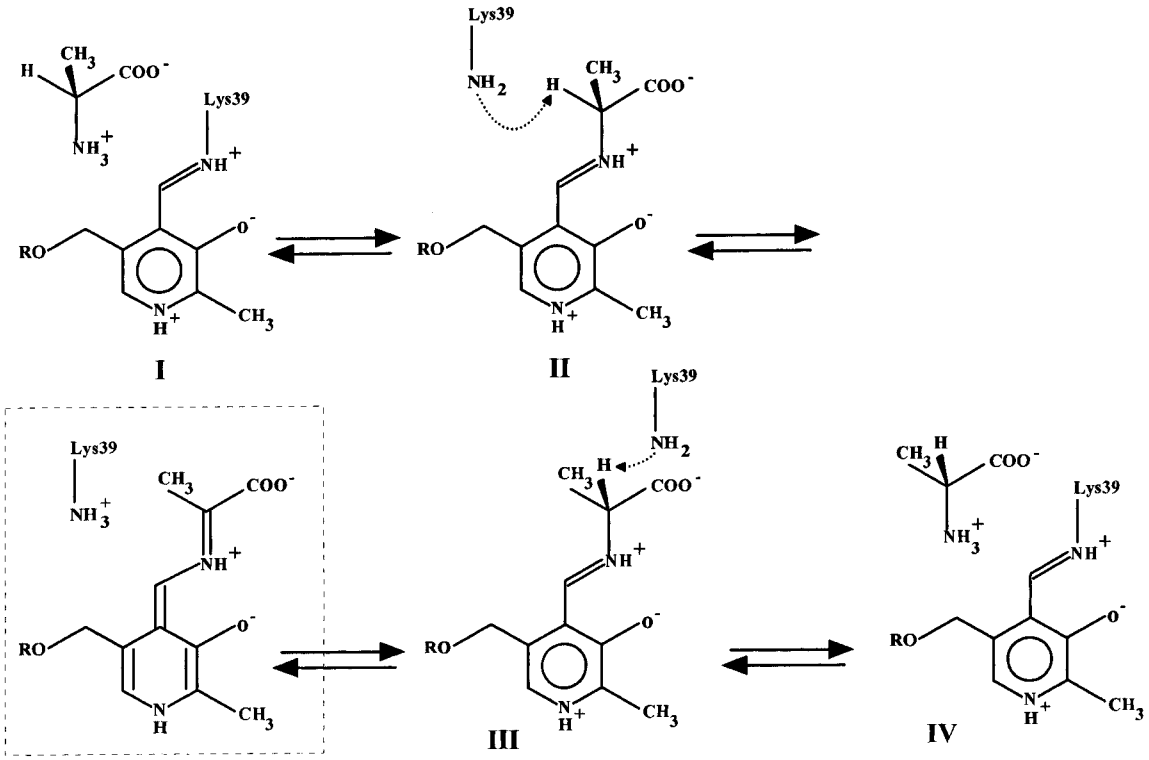

FIGURE 7: Postulated mechanism of alanine racemase. The mechanism shown implies a one-base mechanism with base/acid in the active site. That may not be true and another residue may play this role as well, resulting in a two-base mechanism. There is no obvious residue in the structure to support this latter hypothesis. The intermediate quinonoid structure is displayed within the dashed lines to indicate its hypothetical character.

domain of alanine racemase were classical α/β barrel proteins. These are, in order of descending similarity: triosephosphate isomerase (Wierenga *et al.*, 1991), trimethylamine dehydrogenase (Lim *et al.*, 1986), ribulose-1,5-bisphosphate carboxylase/oxgenase (Curmi *et al.*, 1992), fructose-1,6-bisphosphate aldolase (Hester *et al.*, 1991), and xylose isomerase (Lavie *et al.*, 1994). The C-terminal domain, on the other hand, bore far less similarity to any protein, and the highest scoring structural motifs were either ferredoxin reductases, phthalate dioxygenase reductase (Correll *et al.*, 1992), ferredoxin:$NADP^+$ oxidoreductase (Karplus *et al.*, 1991), or serine proteases (Tsunasawa *et al.*, 1989, Fujinaga *et al.*, 1985). There is, however, no obvious relationship between the structure of the second domain and the functions of these proteins.

The racemization of alanine by alanine racemase is believed to proceed via the following steps (see Figure 7): (i) the initial transaldimination, during which the Lys39 residue, which is covalently bound to the PLP cofactor, is displaced by the incoming amino group of the alanine substrate; (ii) abstraction of the α-proton, which could produce a "quinonoid" resonance-stabilized carbanion intermediate; (iii) reprotonation either on the opposite side of the α-carbon carbanion, to produce the opposite enantiomer of the alanine substrate, or reprotonation on the original side of the carbanion, presumably by the protonated Lys39 ϵ-amino group, giving rise to the same enantiomer of alanine as that of the substrate; and (iv) release of the alanine product.

These catalytic steps, abstraction of a proton and reprotonation, must also be part of the mechanism of all other PLP-containing enzymes, and thus the reaction catalyzed by alanine racemase represents the simplest of this class of enzymes. The structures of the active sites of several pyridoxal 5′-phosphate-containing enzymes have been elucidated. These proteins include aspartate aminotransferase (Kirsch *et al.*, 1984; Ford *et al.*, 1980; Almo *et al.*, 1994), D-amino acid aminotransferase (Sugio *et al.*, 1995), dialkylglycine decarboxylase (Toney *et al.*, 1993), tryptophan synthase from *Salmonella typhimurium* (Hyde *et al.*, 1988), and tyrosine−phenol lyase (Antson *et al.*, 1992, 1993). These proteins catalyze a variety of different reactions. Dialkylglycine decarboxylase from *Pseudomonas cepecia* is a pyridoxal 5′-phosphate-dependent enzyme that is unusual in catalyzing both decarboxylation and transamination in its catalytic cycle (Keller *et al.*, 1990). In the first half of the catalytic cycle, dialkylglycines such as α-methylalanine are oxidatively decarboxylated to give CO_2 and a ketone, with the amino group remaining on the pyridoxamine. The second half-cycle is a normal transamination, with pyruvate as the substrate. Tyrosine−phenol lyase (E.C. 4.1.99.2) is a pyridoxal 5′-phosphate-dependent enzyme which catalyzes the α-elimination of L-tyrosine to give phenol and ammonium pyruvate (Kumagai *et al.*, 1970a,b). The bacterial tryptophan synthase (E.C. 4.2.1.20) is a bienzyme complex composed of subunits α and β, which catalyzes the final two steps of L-tryptophan biosynthesis (Hyde *et al.*, 1988). The structures of the active sites of these PLP enzymes are quite similar (with the possible exception of the tryptophan synthase β-subunit), despite the different reactions they catalyze. The structures of the active sites of both dialkylglycine decarboxylase and tyrosine−phenol lyase greatly resemble that of aspartate aminotransferase (E.C. 2.6.1.1), which is the best studied of these enzymes and catalyzes the reversible interconversion of dicarboxylic amino and keto acids.

Aspartate aminotransferases from a variety of sources have been isolated and characterized, and their structures have been elucidated. Among the best characterized are the mitochondrial aspartate aminotransferase (Ford *et al.*, 1980;

Kirsch *et al*., 1984) and the *E. coli* enzyme (Almo *et al.*, 1994). One of the most important and best studied interactions between the coenzyme and the protein active site of all PLP enzymes is that between the protonated pyridine nitrogen of PLP and an amino acid side chain. In L-Asp-AT , this interaction is a hydrogen bond/salt bridge between the N1 proton of PLP and a negatively charged aspartate side chain (Asp222 in *E. coli*, Asp258 in the mitochondrial enzyme). In DGD (Toney *et al.*, 1993) this aspartate residue is conserved (Asp243). It would also appear to be conserved in tyrosine−phenol lyase (Asp214), although the electron density in the active site was not well-defined, and the structure was determined of the apoenzyme (Antson *et al*., 1993). In alanine racemase, the negatively charged aspartate residue is replaced by a positively charged arginine (Arg219). This difference can be expected to have important implications on the electronic distribution of the PLP-alanine adduct, and thereby on the type and rate of the reaction which will occur on the alanine substrate. It is noteworthy that, in the structure of the β-subunit of tryptophan synthase, the aspartate residue is replaced either by a cysteine or a serine, in either case a neutral side chain (Hyde *et al.*, 1988). In fact, among the PLP enzymes whose structures are known, the presence of a negatively charged side chain interacting with the N1 proton of PLP has been demonstrated in only those enzymes whose catalytic cycle involves release of a keto acid (tyrosine−phenol lyase, L-Asp-AT, and DAAT) or a ketone (DGD), requiring the formation of a ketimine intermediate. Those enzymes that do not release an oxo intermediate (tryptophan synthase and alanine racemase) contain interactions between neutral or positively charged side chains and the N1 proton of PLP. The hydrogen-bonded salt bridge between the aspartate side chain of the former group of PLP enzymes and the N1 proton is believed to stabilize the carbanion intermediates of the reactions, since the protonated form of the pyridine ring of PLP, which is stabilized by this interaction, will behave as an electron sink.

The importance of this interaction between the N1 proton and the aspartate residue side chain has been studied in the case of the *E. coli* L-Asp-AT , in which Asp222 was mutated either to an alanine residue (Onuffer & Kirsch, 1994) or a variety of amino acid resides (Yano *et al.*, 1992). An Asp222Glu mutation did not have any important effects on enzyme activity and behaved as a conservative mutation. Asp222Ala and Asp222Asn mutants displayed an important decrease in apparent transaminase activity, especially in the reaction with the aspartate substrate. In the case of the Asp222Ala, the kinetic data of the first half-reaction suggested that the overall equilibrium of the reaction had been shifted far toward the side of PLP and aspartate, in comparison with the wild-type enzyme. In this respect, it resembles alanine racemase, whose equilibrium is so much in favor of PLP and alanine that there is essentially no formation of pyruvate and ammonium. Furthermore, the forward reaction of the Asp222Ala mutant was biphasic, with a fast reaction whose rate varied with substrate concentration, and a slow reaction whose rate did not. This indicates that the abstraction of the α-proton of the substrate is the rate-limiting step in the reaction catalyzed by this mutant, while it is only partially rate-limiting for the wild-type enzyme (Onuffer & Kirsch, 1994). It was determined that the presence of the Asp222 residue facilitates the removal of the α-proton by as much as 5 kcal mol^{-1}. However, the abstraction of the α-proton from the PLP-alanine adduct in alanine racemase is not the rate-limiting step in either the D-alanine or L-alanine direction (Faraci & Walsh, 1988)

It is believed that this interaction between the N1 proton and a negatively charged side chain will have two, possibly three, important effects. First, the protonated state of the pyridine nitrogen reduces the pK_a of the imine nitrogen of the internal aldimine by approximately 2.5 units (Christen & Metzler, 1985). This would cause the imine nitrogen to be relatively unprotonated under conditions where the incoming amino acid substrate amino group is protonated, thereby allowing efficient transaldimination to occur. It is therefore probable that, in the case of alanine racemase, this imine nitrogen will be relatively protonated (since the pyridine nitrogen is relatively unprotonated) and that transaldimination will be relatively inefficient. In fact, it has been postulated that transaldimination is the rate-limiting step in the racemization of either D-alanine or L-alanine by alanine racemase (Faraci & Walsh, 1988). Thus, the difference in the rate-limiting step of alanine racemase and L-Asp-AT may be due in part to the presence of a positively charged arginine binding to the N1 proton.

The second effect caused by hydrogen bonding of the N1 proton by Asp222 of L-Asp-AT is an increase of the pK_a of the pyridine nitrogen proton, which results in the nitrogen remaining protonated and in the cofactor functioning as a more efficient electron sink during both α-proton abstraction and in the subsequent 1,3-prototropic shift. In alanine racemase, this pyridine nitrogen will be relatively less protonated than in L-Asp-AT , implying that the 1,3-prototrophic shift can be expected to occur much less efficiently and the postulated quinonoid intermediate will be severely destabilized (see Figure 7).

A third possible effect concerns the domain closure event in L-Asp-AT . The Asp222Ala mutant displayed an unusual negative cooperativity, which was interpreted as two slowly interconverting forms of the enzyme, only one of which was catalytically active (Onuffer & Kirsch, 1994). It was concluded that this slow transition was associated with domain closure, an event known to occur in L-Asp-AT upon binding of substrate or inhibitors. As mentioned previously, there is evidence that alanine racemase also undergoes an important conformational change upon substrate binding. Whether Arg219 also plays a role in this change is not known.

Another interaction between the PLP cofactor and an active-site side chain involves the hydroxyl group of PLP. The pK_a of this hydroxyl is very low and it is therefore unprotonated. In L-Asp-AT , this hydroxylate ion receives a hydrogen bond from the hydroxyl group of Tyr225 (Goldberg *et al.*, 1991) in the unprotonated PLP form (no proton on the imine nitrogen of the internal aldimine; this is the active form of the enzyme). When the imine nitrogen is protonated, it preferentially forms a hydrogen bond with the O3′ moiety of PLP. In tyrosine−phenol lyase, the nature of the interaction between the O3′ hydroxylate ion and an amino acid side chain is unclear (this is the apoenzyme). In the case of DGD there is a definite interaction between the O3′ hydroxylate and Gln246, while in the tryptophan synthase β-subunit it would appear that there is no interaction of the protein with O3′, although the poorly localized Gln114 may fulfill this role. In alanine racemase it is the NH2 of the guanidine side chain of Arg136 which would appear to

donate a hydrogen bond to the O3′ hydroxyl ion (see Figures 5 and 6). Thus the nature of the residue interacting with the O3′ hydroxylate is quite variable and is expected to influence the electronic distribution on the PLP moiety, as has been shown in the case of L-Asp-AT .

When the Tyr225 in L-Asp-AT is replaced by a phenylalanine, the pK_a of the imine nitrogen is increased by 1.7 units, which is probably due to the loss of the stabilization provided by the hydrogen bond (Deng *et al.*, 1993). It is evident that two interactions in L-Asp-AT contribute to maintaining the low pK_a of the imine nitrogen: one between Asp222 and the pyridine N1 proton, and one between Tyr225 and the PLP O3′. While the first of these is lacking in alanine racemase, it is probable that the second is as well, further supporting the belief that transaldimination is the rate-limiting step of alanine racemase. The hydrogen bond between Tyr225 and the O3′ of PLP has another effect in L-Asp-AT which may be of importance in alanine racemase. The presence of this interaction causes an increase in the k_{cat} of the transamination reaction, due to an apparent stabilization of the free unliganded form of the protein. The Tyr225Phe mutant displayed increased values of V/K and k_{cat}, presumably because the lack of a hydrogen bond allowed the PLP to adopt a conformation which stabilized the enzyme−substrate complex. Efforts are now underway to determine the structure of alanine racemase with alanine bound in the active site in order to determine whether Arg136 plays the same role in alanine racemase as Tyr225 plays in L-Asp-AT.

When the pyridoxal 5′-phosphate molecules in the active sites of alanine racemase and L-Asp-AT are superimposed, the geometry of their binding is quite different. In the case of alanine racemase, the Lys39 side chain comes from one side of the PLP aromatic ring, whereas in L-Asp-AT, the Lys258 side chain comes from the opposite side of the ring. In L-Asp-AT, Lys258 approaches the coenzyme from the *si* face and thereby contributes to the strict stereospecificity of proton exchange at the C4′ of PLP, since the Schiff base is oriented in such a way that the α-proton faces the protein and addition of a proton to the ketimine intermediate results in the formation of an L-amino acid. When the PLP molecules of alanine racemase and of D-amino acid aminotransferase (Sugio *et al.*, 1995) are superimposed, the position of the PLP-binding lysines are very similar. The lysine in DAAT approaches the *re* face of the PLP cofactor and thereby catalyzes *pro-R* proton transfer at C4′ (the opposite of that for L-Asp-AT). Thus, it would appear that Lys39 in alanine racemase also approaches the *re* face of PLP. The PLP molecules of these three proteins superimpose quite well (despite large differences in the relative positions of the phosphate group). The active sites of both alanine racemase and L-ASP-AT contain a hydrophobic region on one side of the PLP ring; in this case the hydrophobic pockets are on the same side of the PLP ring. The bulky hydrophobic residue Trp140 in L-ASP-AT is roughly in the same position as the Leu85 and Val37 residues in alanine racemase. The side chains of the residues interacting with the O3′ hydroxylate group of PLP (Arg136 in BSAR and Tyr225 in L-Asp-AT) are in similar positions. The α-carbons of the side chains interacting with the N1 proton of PLP (Arg219 in BSAR and Asp222 in L-Asp-AT) are on opposite sides of the N1 nitrogen, but the guanidinium and carboxylate groups are in roughly the same positions. It is in the binding to the lysine side chain and the relative position of the phosphate group that the active sites show the greatest difference in geometry.

The sequence alignment of the four anabolic alanine racemases [from *B. stearothermophilus* (Tanizawa *et al.*, 1988), *B. subtilis* (Ferrari *et al.*, 1985), *E. coli* (Blattner *et al.*, 1993), and *S. typhimurium* (Galakatos *et al.*, 1986)] and two catabolic alanine racemases [from *E. coli* (Lobocka *et al.*, 1994) and *S. typhimurium* (Wasserman *et al.*, 1984)] reveals a high level of amino acid identity (17.5% of amino acid residues are strictly conserved among all the racemases, while 22% of the residues are conserved among catabolic alanine racemases). Most notably, the Arg219 residue is conserved in all four alanine racemases, as are several other residues which may be implicated in activity. The examination of the positions of those residues that are conserved in all anabolic alanine racemases did confirm the role played by many of them. The most important stretch of conserved residues is that following the active-site Lys39, from residues 40 to 47. The roles of Ala40 and Ala42 are not clear, and are probably structural. However, Asn41 forms several important interactions: the OD1 forms a hydrogen bond with the NH2 of Arg378 (3.1 Å) and with the main-chain N of Asp47 (2.9 Å), while the ND2 would appear to bind a water molecule (3.0 Å). The OH group of Tyr43 binds to one of the oxygen atoms of the phosphate group of PLP (2.7 Å). The main-chain NH of His45 forms a hydrogen bond with the main-chain O of Ala42 (3.2 Å), and the NE2 binds a water molecule (3.1 Å), which also interacts with the main-chain O of Tyr225. Thus, the three charged residues within the conserved eight amino acid stretch are involved in maintaining the geometry of the active sites of these alanine racemases.

Asp68 is an interface residue between subunits and is conserved as an acidic residue in all alanine racemases. One of the side-chain carboxylate oxygens of Asp68 forms a hydrogen bond with the Asn379′ (3.2 Å), and the other with the main-chain N of His5′ (3.0 Å). The following amino acid residue is a glutamate in all alanine racemases (Glu69 in BSAR) and its OE2 forms a hydrogen bond (2.9 Å) with NH1 of Arg363′ (also conserved in all alanine racemases, see below), while the OE1 forms a hydrogen bond with the main-chain N of Ala65 (2.8 Å). Arg74 is also strictly conserved among all alanine racemases. It would appear to play a role in maintaining the structure of the α/β barrel, since it intercalates between β-strands B4 and B5 and interacts with side chains from both strands [the NE hydrogen-bonds with the main-chain O of Gln99 (2.7 Å), the NH2 hydrogen-bonds with the main-chain O of Ala80 (2.9 Å), while the NH1 hydrogen-bonds with the main-chain O of Ile78 (2.8 Å)].

Another long stretch of highly conserved amino acid residues runs from Lys129 to Lys140. Lys129 is strictly conserved among all alanine racemases, but its role is unclear. It lies in the active site but would appear to interact only with a pair of water molecules. Its role may be clarified when the structure of the alanine-bound alanine racemase is available. Asp131 is conserved among the anabolic alanine racemases, while being conservatively replaced by asparagine in the catabolic racemases. The OD1 of the side chain forms a hydrogen bond with the main-chain N of Met134 (3.1 Å), which lies close to the active site but whose role is unclear. Thr132 is replaced by serine in the catabolic racemases, and

its OG1 forms a hydrogen bond (3.0 Å) with the OG1 of Thr165 (which is conserved either as a threonine or as a serine in all racemases) and with the NE2 of Gln181 (also conserved among the anabolic racemases but replaced with arginine and alanine in the catabolic racemases from *E. coli* and *S. typhimurium*, respectively). This is one of the rare examples of a residue with an important interaction which is not strictly conserved among all the racemases.

Arg136, which plays a definite role in the active site by donating a hydrogen bond to the O3′ hydroxylate ion of PLP (as well as possibly binding to the carboxylate group of the substrate alanine), is strictly conserved among all alanine racemases, as is Met134, which is also in the active-site pocket and whose role is not clear. Lys140 is conserved as a polar residue among all alanine racemases (lysine in anabolic enzymes from *B. stearothermophilus* and *B. subtilis*, arginine in the *E. coli* and *S. typhimurium* anabolic enzymes, and glutamine in the *E. coli* and *S. typhimurium* catabolic enzymes). In *B. stearothermophilus*, the amino group of the Lys140 side chain forms a hydrogen bond with the acidic side chain of Glu261′ from the other monomer (3.0 Å). This Glu261 is strictly conserved among all alanine racemases. This interaction is one of the few intersubunit salt bridges.

His166 is strictly conserved among all alanine racemases (it is part of the hydrogen-bonding network described above), as are Phe167 and Ala168. Thr165 is conserved as either threonine or serine among all the racemases and was described above. An acidic residue is always present at position 171 (aspartate in anabolic alanine racemases, glutamate in the catabolic ones) and lies at the external entrance (solvent side) of the α/β barrel. Glu172 is also present in all the anabolic racemases but is replaced by histidine in the catabolic ones. Ser204 is conserved in all alanine racemases and forms a hydrogen bond with one of the oxygen atoms of the phosphate group of PLP. Arg219 is also strictly conserved (interacts with the N1 of PLP), as is Tyr225, whose OH group apparently forms a hydrogen bond (2.8 Å) with the main-chain O of Val37 (part of the very highly conserved sequence around the PLP-binding Lys39). Ser249 is strictly conserved among all alanine racemases, and its OG interacts (3.0 Å) with the OG1 of Thr8 (which is not conserved!). Tyr265, whose OH group forms a hydrogen bond with His166, is also strictly conserved among all alanine racemases.

A number of other conserved residues do not interact with the cofactor directly but do contribute to the active-site geometry. A region with a high number of strictly conserved amino acid residues runs from Gly283 to Trp288 (this is the tryptophan which was inserted into the sequence on the basis of the observed electron density and whose presence was subsequently confirmed by the sequencing of the structural gene). Tyr284 lies within this highly conserved region and lies within the active site of the other monomer. What role it may play in binding or catalysis is unclear, however. On the other hand, the role that the strictly conserved Asp286 plays is much more evident. The OD2 of Asp286 forms a hydrogen bond with the main-chain N of Gly283 (also strictly conserved) and with the NH1 of Arg6 (conserved except in the case of the anabolic enzymes from *E. coli* and *S. typhimurium*, in which this residue is a glutamine). The net effect is the stabilization of the loop from which Tyr 284 originates. Met312 and Asp313 are strictly conserved in all alanine racemases. Both lie in the active site of the other monomer. The role of Met312 is unclear, but Asp313 lies close to the NE of Lys39′ and may bind the latter when it is released upon binding of alanine (see above). Interestingly, Gln314, which would appear to play a role in the active site of the other monomer (interaction with Arg136′), is present only in the *B. stearothermophilus* and *B. subtilis* enzymes and is a methionine in all the other alanine racemases. Tyr354 is strictly conserved (OH group binds to oxygen of phosphate group of PLP), as is Glu355. Glu355 must play a structural role, since its OE1 tightly binds two water molecules, while the OE2 forms a hydrogen bond with the main-chain N of Arg290 (which is conserved among all alanine racemases with the exception of the anabolic enzyme from *E. coli*). Arg363 is strictly conserved among all alanine racemases. The NH2 of Arg363 forms a hydrogen bond with the OD1 of Asp313 (2.7 Å) and with the OD2 of Asp286 (3.0 Å), while the NH1 forms hydrogen bonds with the OE2 of Glu69′ (3.1 Å) and with the OD1 of Asp313 (2.8 Å). This is obviously an important interaction, due to the expected role of Asp313.

The large majority of the amino acid residues whose possible role in either protein structure, substrate or cofactor binding, and catalysis has been tentatively identified are conserved among all the alanine racemases, even if the overall identity among these racemases is poor. This suggests that all of the proteins are derived from a single ancestral protein and that the differences among these proteins lie in regions of lesser importance for catalysis. However, it also casts doubt on the assertions that the *S. typhimurium* enzymes are monomeric (Esaki & Walsh, 1986), as opposed to the *B. stearothermophilus* enzyme, which is homodimeric. If one accepts that the structure of all these alanine racemases is very similar, based on the conservation of almost every amino acid residue implicated in structure or catalysis, it is difficult to imagine that residues from one monomer which are part of the active site of the other monomer (such as Tyr265, Asp313, Met312, and Arg363) would have been conserved in an enzyme which was monomeric and therefore had no use for these residues. This would seem to imply either that the monomeric enzymes adopt a very different structure, which would allow these conserved residues to play a role in the monomeric protein, or that these enzymes are actually dimeric, and their structure is very similar to that of the alanine racemase from *B. stearothermophilus*. The other, unlikely possibility is that none of these enzymes are dimers and that the dimer structure obtained by crystallography is a result of crystal packing and not the natural condition of the enzyme. However, it is interesting to note that very few of the residues whose side chains may play a role in maintaining the dimer structure of alanine racemase through hydrogen bonding or salt bridges are conserved. Of these interactions, described above, only the interaction between the NE of Lys140 (arginine in *E. coli* and *S. typhimurium*) and the OE2 of Glu261 and that between the NE2 of His166 and the OH of Tyr265 are conserved. Several of the interactions between a side-chain and a main-chain atom are maintained. It is nonetheless most likely that all these enzymes are dimeric, and the results obtained in the proteolytic digestions described below, together with the newly obtained structure of one of these enzymes, appear to confirm this hypothesis.

When certain alanine racemases were subjected to proteolytic cleavage with specific or nonspecific proteases, a short polypeptide sequence was excised from the protein, giving rise to an alanine racemase composed of two separate polypeptides (Galakatos & Walsh, 1986). The hydrolyzed portion of the protein (four amino acid residues) was postulated to be part of an interdomain hinge, which is conserved among all known alanine racemases and is essential for a catalytically efficient enzyme. In the case of alanine racemase from *B. stearothermophilus*, the proteolysis gave rise to a fragmentation pattern which closely resembled that of the other alanine racemases studied (Galakatos & Walsh, 1986), although the peptide cleaved away from the intact molecule was not identified. The peptide which was cleaved away was identified in the case of *S. typhimurium* Alr (which is the biosynthetic form of the *S. typhimurium* enzyme and therefore corresponds to the alanine racemase from *B. stearothermophilus* discussed here) as G^{256}-G-T-W^{259}. This corresponds to residues G^{266}-A-T-Y^{269} in the *B. stearothermophilus* enzyme. The first glycine of these two peptides is conserved in all the biosynthetic enzymes sequenced and may play a structural role, since glycine residues are unique in having greater flexibility in the polypeptide chain than other residues. When this tetrapeptide was excised from the Alr alanine racemase, the enzyme retained *ca.* 3% of its initial activity. Furthermore, the two polypeptides did not disassociate under nondenaturing conditions. In the case of the DadB alanine racemase (the catabolic alanine racemase of *S. typhimurium*) it was also demonstrated that 76% of the active sites were still present. It was concluded that this tetrapeptide in the DadB and Alr alanine racemases was an interdomain hinge, which when cleaved away did not greatly disturb the active-site geometry although the catalytic efficiency of the enzymes was greatly reduced. A similar study was performed on the *B. stearothermophilus* enzyme, but in this case, the two fragments of the proteins were produced as separate polypeptides by introducing a new stop codon, a ribosomal binding site, and a new initiation codon between residues Tyr269 and Thr270 (Toyama *et al.*, 1991). This protein was active, but the K_m for D-alanine increased 2.2-fold, and the V_{max} of the fragmentary enzyme was reduced by 2-fold. The kinetic constants in the L-alanine to D-alanine direction were similarly affected. It was also demonstrated that expression of the two fragmentary polypeptides resulted in an active alanine racemase only when they were coexpressed (Toyama *et al.*, 1991) but that the secondary structure of the active fragmentary enzyme was essentially that of native alanine racemase. In the light of the structure of the alanine racemase from *B. stearothermophilus*, the possible role of the excised region can be explained.

The corresponding region in the *B. stearothermophilus* enzyme lies at the C-terminal end of the interdomain linker (between the α/β barrel and the second domain), actually at the C-terminal end of the first β-strand after the linker (see Figures 1, 2, and 5). This β-strand starts at the point of the monomer furthest from the α/β barrel and heads back from this extreme end toward the α/β barrel. The four amino acid residues which correspond to those excised in the *S. typhimurium* proteins lie at the end of the β-strand in a turn before the second β-strand of the second domain (see Figure 5). This region lies at the monomer−monomer interface and is on the surface of the molecule. It is not evident what catalytic role the four excised residues could play, since they are not near the active site of the protein, nor do they form any interactions which could be important in maintaining the secondary structure of the protein.

On the basis of the structure of alanine racemase, it is our belief that the important residue in this region is actually Tyr265, which would correspond to the residue whose peptide bond with the first glycine was cleaved in the two *S. typhimurium* enzymes. It would thus be the C-terminal residue of the large domain after cleavage. This Tyr265 is one of the very few amino acid side chains of one monomer which appear to play a role the active site of the other monomer. The OH group of Tyr265 lies 2.8 Å from the NE2 of His166 of the other monomer. This His166 plays an important role in the structure of the active site, since the ND1 forms a hydrogen bond with the NH2 of the guanidinium group of Arg219, which forms a hydrogen bond with the pyridine nitrogen of the pyridoxal 5′-phosphate cofactor. Assuming that the binding site of the acetate molecule in the active site corresponds to that of alanine during catalysis, it would appear that the Tyr265 may also play a role in catalysis. After proton abstraction, it is believed that the protonated Lys39 side chain may be responsible for the protonation of the alanine-pyridoxal 5′-phosphate quinonoid intermediate. Reprotonation by Lys39 would regenerate the same enantiomer of alanine as the initial substrate. In order for racemization to occur, the proton donor should lie on the opposite side of the C carbon (which is postulated to lie where the methyl group of the acetate molecule lies). The side chain which lies almost directly opposite the Lys39 side chain is that of Tyr265. It is therefore possible that the OH group of Tyr265 is the putative second base believed to exist in the active site of alanine racemase.

The structure of alanine racemase has for the first time revealed the presence of pyridoxal 5′-phosphate in α/β barrel structural motifs and emphasizes the catalytic flexibility of this structural motif. The postulated two-domain structure connected by a hinge (Galakatos & Walsh, 1986, 1989) has been confirmed, although the location of this hinge is different than that expected. The structure of the active site has provided clues to the mechanism of racemization and how secondary pyridoxal 5′-phosphate-dependent reactions are avoided.

ACKNOWLEDGMENT

We thank Lynne Rardin, David H. Harrison, and Marty Stanton for assistance and helpful discussions. The assistance of Liisa Holm (EMBL, Heidelberg) in the Dali structural similarity search and B. Rost (EMBL, Heidelberg) in the secondary structure prediction is gratefully acknowledged. The *E. coli* strain W3110 containing pMDalr3 was obtained from the laboratory of Professor C. T. Walsh (Harvard Medical School). The contribution of the Glaxo Institute for Molecular Biology in resequencing parts of the gene of alanine racemase is gratefully acknowledged. We are grateful to Ezra Peisach and Anthony Morollo for help with the figures.

REFERENCES

Adams, E. (1976) *Adv. Enzymol. Relat. Areas Mol. Biol. 44*, 69−138.

Almo, S. L., Smith, D. L., Danishefsky, A. T., & Ringe, D. (1994) *Protein Eng. 7*, 405−412.

Antson, A. A., Strokopytov, B. V., Murshudov, G. N., Isupov, M. N., Harutyunyan, E. H., Demidkina, T. V., Vassylyev, D. G., Dauter, Z., Terry, H., & Wilson, K. S. (1992) *FEBS Lett. 302*, 256−260.

Antson, A. A., Demidkina, T. V., Gollnick, P., Dauter, Z., Von Tersch, R. L., Long, J., Berezhnoy, S. N., Phillips, R. S., Harutyunyan, E. H., & Wilson, K. S. (1993) *Biochemistry 32*, 4195−4206.

Blattner, F. R., Burland, V. D., Plunkett, G., III, Sofia, H. J., & Daniels, D. L. (1993) *Nucleic Acids Res. 21*, 5408−5417.

Brünger, A. T. (1992) *X-PLOR, A System for X-ray Crystallography and NMR*, Version 3.1, Yale University Press, New Haven, CT.

Christen, P., & Metzler, D., Eds. (1985) *Transaminases*, Wiley & Sons, New York.

Copié, V., Faraci, W. S., Walsh, C. T., & Griffin, R. G. (1988) *Biochemistry 27*, 4966−4970.

Correll, C. C., Batie, C. J., Ballou, D. P., & Ludwig, M. L. (1992) *Science 258*, 1604−1610.

Curmi, P. M. G., Cascio, D., Sweet, R. M., Eisenberg, D., & Schreuder, H. (1992) *J. Biol. Chem. 267*, 16980−16989.

Deng, H., Goldberg, J. M., Kirsch, J., & Callender R. (1993) *J. Am. Chem. Soc. 115*, 8869.

Diven, W. F., Scholz, J. J., & Johnson, R. B. (1964) *Biochim. Biophys. Acta 85*, 322.

Erion, M. D., & Walsh, C. T. (1987) *Biochemistry 26*, 3417−3425.

Esaki, N., & Walsh, C. T. (1986) *Biochemistry 25*, 3261−3267.

Fan, C, Moews, P. C., Walsh, C. T., & Knox, J. R. (1994) *Science 266*, 439−443.

Faraci, S. W., & Walsh, C. T. (1988) *Biochemistry 27*, 3267−3276.

Farber, G. K., & Petsko, G. A. (1990) *Trends Biochem. Sci. 15*, 228−234.

Ferrari, E., Henner, D. J., & Yang, M. Y. (1985) *Bio/Technology 3*, 1003−1007.

Ford, G. C., Eichele, G., & Jansonius, J. N. (1980) *Proc. Natl. Acad. Sci. U.S.A. 77*, 2559−2563.

Fujinaga, M., DelBaere, L. T. J., Brayer, G. D., & James, M. N. G. (1985) *J. Mol. Biol. 184*, 479−502.

Galakatos, N. G., & Walsh, C. T. (1987) *Biochemistry 26*, 8475−8480.

Galakatos, N. G., & Walsh, C. T. (1989) *Biochemistry 28*, 8167−8174.

Galakatos, N. G., Daub, E., Botstein, D., & Walsh, C. T. (1986) *Biochemistry 25*, 3255−3260.

Goldberg, J. M., Swanson, R. V., Goodman, H. S., & Kirsch, J. F. (1991) *Biochemistry 30*, 305−312.

Hendrikson, W. (1979) *Acta Crystallogr. A35*, 158−163.

Hester, G., Brenner-Holzach, O., Rossi, F. A., Struck-Donatz, M., Winterhalter, K. H., Smit, J. D. G., & Piontek, K. (1991) *FEBS Lett. 292*, 237−242.

Hoffmann, K., Schneider-Scherzer, E., Kleinkauf, H., & Zocher, R. (1994) *J. Biol. Chem. 269*, 12710−12714.

Holm, L., & Sander, C. (1993) *J. Mol. Biol. 233*, 123−138.

Holm, L., Ouzounis, C., Tuparev, G., Vriend, G., & Sander, C. (1992) *Protein Sci. 1*, 1691−1698.

Hyde, C. C., Ahmed, S. A., Padlan, E. A., Miles, E. W., & Davies, D. R. (1988) *J. Biol. Chem. 263*, 17857−17871.

Inagaki, K., Tanizawa, K., Badet, B., Walsh, C. T., Tanaka, H., & Soda, K. (1986) *Biochemistry 25*, 3268−3274.

Jones, T. A. (1992) *Molecular Replacement* (Dodson, E. J., Glover, S., & Wolf, W., Eds.) pp 92−105, SERC Daresbury Laboratory, Daresbury, U.K.

Jones, T. A., Zou, J. Y., Cowan, S. W., & Kjeldgaard, M. (1991) *Acta Crystallogr. A47*, 110−119.

Kabsch, W., Mannherz, H. G., Suck, D., Pai, E. F., & Holmes, K. C. (1990) *Nature 347*, 37−44.

Kaczorowski, G., Shaw, L., Fuentes, M., &Walsh, C. T. (1975a) *J. Biol. Chem. 250*, 2855−2865.

Kaczorowski, G., Shaw, L., Laura, R., & Walsh, C. T. (1975b) *J. Biol. Chem. 250*, 8921−8930.

Karplus, P. A., Daniels, M. J., & Herriott, J. R. (1991) *Science 251*, 60−66.

Keller, J. W., Baurick, K. B., Rutt, G. C., O'Malley, M. W., Sonafrank, N. L., Reynolds, R. A., Ebbesson, L. O., & Vajdos, F. F. (1990) *J. Biol. Chem. 265*, 5531−5539.

Kirsch, J. F., Eichele, G., Ford, G. C., Vincent, M. G., & Jansonius, J. N. (1984) *J. Mol. Biol. 174*, 497−525.

Kleywegt, G. J., & Jones, T. A. (1994) in *From First Map to Final Model* (Dodson, E. J., Glover, S., & Wolf, W., Eds.) pp 59−66, SERC Daresbury Laboratory, Daresbury, U.K.

Kumagai, H., Yamada, H., Matsui, H., Oshkishi, H., & Ogata, K. (1970a) *J. Biol. Chem. 245*, 1767−1772.

Kumagai, H., Yamada, H., Matsui, H., Oshkishi, H., & Ogata, K. (1970b) *J. Biol. Chem. 245*, 1773−1777.

Lambert, M. P., & Neuhaus, F. C. (1972) *J. Bacteriol. 110*, 978−987.

Lavie, A., Allen, K. N., Petsko, G. A., & Ringe, D. (1994) *Biochemistry 33*, 5469−5480.

Lim, L. W., Shamala, N., Matthews, F. S., Steenkamp, D. J., Hamlin, R., & Xuong, N. H. (1986) *J. Biol. Chem. 261*, 15140−15146.

Lobocka, M. B., Hennig, J., Wild, J., & Klopotowski, T. (1994) *J. Bacteriol. 176*, 1500−1510.

Neidhart, D. J., Distefano, M. D., Tanizawa, K., Soda, K., Walsh, C. T., & Petsko, G. A. (1987) *J. Biol. Chem. 262*, 15323−15326.

Neuhaus, F. C. (1967) in *Antibiotics: Mechanism of Action* (Gottleib, D., & Shaw, P. D., Eds.) Vol. 1, p 40, Springer-Verlag, New York.

Onuffer, J. J., & Kirsch, J. F. (1994) *Protein Eng. 7*, 413−424.

Rosso, G., Takashima, K., & Adams, E. (1969) *Biochem. Biophys. Res. Commun. 34*, 134−140.

Rost. B., & Sander, C. (1993) *J. Mol. Biol. 232*, 584−599.

Rost, B., & Sander, C. (1994) *Proteins: Struct., Funct., Genet. 19*, 55−72.

Sheldrick, G. M. (1985) in *Crystallographic Computing 3* (Sheldrick, G. M., Krüger, C., & Goddard, R. Eds.) p 175, Oxford University Press, Oxford, England.

Sugio, S., Petsko, G. A., Manning, J. M., Soda, K., & Ringe, D. (1995) *Biochemistry 34*, 9661−9669.

Tanizawa, T., Ohshima, A., Scheidegger, A., Inagaki, K., Tanaka, H., & Soda, K. (1988) *Biochemistry 27*, 1311−1316.

Toney, M. D., Hohenester, E., Cowan, S. W., & Jansonius, J. N. (1993) *Science 261*, 756−759.

Toyama, H., Tanizawa, K., Yoshimura, T., Asano, S., Lim, Y.-H., Esaki, N., & Soda, K. (1991) *J. Biol. Chem. 266*, 13634−13639.

Tsunasawa, S., Masaki, T., Hirose, M., Soejima, M., & Sakiyama, F. (1989) *J. Biol. Chem. 264*, 3832−3839.

Wang, E., & Walsh, C. T. (1978) *Biochemistry 17*, 1313−1321.

Wasserman, S. A., Daub, E., Grisafi, P., Botstein, D., & Walsh, C. T. (1984) *Biochemistry 23*, 5182−5187.

Wierenga, R. K., Noble, M. E. M, Vriend, G., Nauche, S., & Hol, W. G. J. (1991) *J. Mol. Biol. 220*, 995−1015.

Wood, W. A., & Gunsalus, I. C. (1951) *J. Biol. Chem. 190*, 403.

Yano, T., Kuramitsu, S., Tanase, S., Morino, Y., & Kagamiyama, H. (1992) *Biochemistry 31*, 5878−5887.

Zhang, K. Y. J. (1993) *Acta Crystallogr. D49*, 213−222.

BI961856C